NASA Technical Memorandum 106911

Design of a Unidirectional Composite Momentum Wheel Rim

Bradley Shogrin
Case Western Reserve University
Cleveland, Ohio

William R. Jones, Jr.
Lewis Research Center
Cleveland, Ohio

and

Joseph M. Prahl
Case Western Reserve University
Cleveland, Ohio

May 1995

National Aeronautics and
Space Administration

DESIGN OF A UNIDIRECTIONAL COMPOSITE MOMENTUM WHEEL RIM

Bradley Shogrin
Department of Mechanical Engineering
Case Western Reserve University
Cleveland, OH 44106

William R. Jones, Jr.
NASA Lewis Research Center
Cleveland, OH 44135

Joseph M. Prahl
Department of Mechanical Engineering
Case Western Reserve University
Cleveland, OH 44106

ABSTRACT

A preliminary study comparing twelve unidirectional-fiber composite systems to five metal materials conventionally used in momentum wheels is presented. Six different fibers are considered in the study; E-Glass, S-Glass, Boron, AS, T300 and Kevlar. Because of the possibility of high momentum requirements, and, thus high stresses, only two matrix materials are considered; a high-modulus (HM) and a intermediate-modulus-high-strength (IMHS) matrix. Each of the six fibers are coupled with each of the two matrix materials. In an effort to optimize the composite system, each composite is considered while varying the fiber volume ratio from 0.0 to 0.7 in increments of 0.1. For fiber volume ratios above 0.2, all twelve unidirectional-fiber composite systems meet the study's requirements with higher factors of safety and less mass than the five conventional isotropic (metal) materials. For example, at a fiber volume ratio of 0.6, the Kevlar/IMHS composite system has a safety factor 4.5 times greater than that of a steel (maraging) system and a $\sim 10\%$ reduction in weight.

INTRODUCTION

Momentum wheels are gyroscopic actuators which operate with constant angular velocity. Momentum wheels are required in all geostationary satellites to offset certain fixed-magnitude-forces which constantly interact with the spacecraft causing it to drift off course. For example, the non-sphericity of the earth introduces such forces which cause spacecraft to drift longitudinally if momentum wheels are not present to counteract them.

The rim of a momentum wheel is typically made of a high performance steel or titanium

alloy. During operation the spin of the momentum wheel results in the stress distribution to be higher in the tangential direction than in the radial direction. This anisotropic stress distribution is accentuated as the rim becomes thinner and thinner in the radial direction. The fact that metals are inherently isotropic inhibits their use and makes them inefficient in such an anisotropic stress environment. A superior material for use in such an environment is a unidirectional composite which would exploit it's anisotropic properties, making the wheel less massive, while capable of delivering the same (or more) angular momentum to the spacecraft.

Inherently, the use of a composite material incorporates unique, new challenges to overcome in the momentum wheel's design. One such problem which has been reported is that radially-thick rimmed wheels made of composites have delaminated due to high radial stresses (1,2) resulting in catastrophic failure of the rim. It has also been reported (3) that in spoked composite rims, high stress concentrations present at the composite/spoke interfaces cause premature failure of the rim. To counterbalance both these effects, it has been suggested and shown (4-6) that using numerous composite rims pressfit into one another both reduces the high radial stresses and eliminates the need for spokes.

Following this thin-rim concept, a radially-thin, spokeless, non-prestressed (no stress induced by pressfitting) single rim is considered. The rim is idealized as a free-floating, spinning rim. The twelve unidirectional-fiber composite systems and five isotropic metals are compared under the same momentum and geometric constraints. Since the final objective is to use the momentum wheel in space, hygral effects on the composite systems are not considered. Furthermore, thermal effects on the composite systems are neglected because it is assumed that the momentum wheel will not experience detrimental temperatures. The labors here are the first in several steps eventually leading to a functional multi-ring composite momentum wheel.

APPROACH

Computer code was generated in Mathcad 5.0© to determine the rim's geometry and weight, and to determine the associated radial and tangential stresses, given the material's properties, and geometric and dynamic constraints. Symbol nomenclature is located in Appendix I.

Material Properties

The relevant properties of the five metals considered: a Titanium Alloy (ZK 60), and four steels: AISI 4340, 18 Ni-250 (maraging), hp 9-4-20, and hp 9-4-30, are shown in Table 1. These were chosen for the study because of their use in high performance flywheels (3), such as momentum wheels. The properties of cast iron (G-15), and carbon steel (Fe 34) are included in Table 1 as a basis for comparison.

The relevant properties of the 6 fiber and 2 matrix types used in this study are seen in Tables 2 and 3, respectively. Each of the six fibers are coupled with each of the two matrix types, constituting 12 composite materials.

The relevant anisotropic properties of each composite, formed by coupling one of the

fibers listed in Table 2 with one of two matrix materials listed in Table 3, and assuming no voids, are given by the following equations (7,8).

Composite density,

$$\rho = \rho_f \cdot (k_f) + \rho_m \cdot (k_m) \tag{1}$$

Where k_f is the fiber volume ratio, and k_m is the resin, or matrix volume ratio and is equal to $(1 - k_f)$.

Composite Modulus of Elasticity in the tangential direction (along the fiber direction, or 11 direction).

$$E_{tang} = E_{c11} = E_{f11} \cdot (k_f) + E_m \cdot (k_m) \tag{2}$$

Composite Modulus of Elasticity in the radial direction (perpendicular to the direction of fiber orientation, or the 22 direction).

$$E_{rad} = E_{c22} = \frac{E_m}{1 - \sqrt{k_f} \cdot (1 - \frac{E_m}{E_{f22}})} \tag{3}$$

Composite longitudinal Poisson's ratio,

$$\nu_{c12} = \nu_{f12} \cdot (k_f) + \nu_m \cdot (k_m) \tag{4}$$

Composite tangential tensile strength,

$$S_{tang} = S_{c11} = S_{f11} \cdot (k_f) \tag{5}$$

The fiber volume ratio is varied from 0.0 (0 % fiber, 100 % matrix) to 0.7 (70 % fiber, 30 % matrix) in increments of 0.1 for each of the 12 composite systems.

Dynamic and Geometric Constraints

Each of the composite and metal materials is considered using the same dynamic and geometric constraints. The wheel's angular momentum (H) is set to 100.0 N*m*sec (73.76 ft*lb_f*sec), the angular velocity (ω) to 628.3 rad/sec (6000 rpm), and inner radius (r_{inner}) and height to 0.30 meters (11.81 inches) and 0.020 meters (0.787 inches), respectively. These values are near or equal to those used in some present momentum wheel designs (9-12).

From the above constraints, and knowing the density of the material (Table 1 for metals, Equation 1 for composites), the outer radius, and total mass of the momentum wheel rim are

obtained as follows.

$$H=\frac{\rho\cdot(r_{outer}^4-r_{inner}^4)\Pi\cdot height\cdot\omega}{2} \tag{6}$$

$$r_{outer}=r_{inner}\cdot\left(1+\frac{2\cdot H}{\rho\cdot\Pi\cdot height\cdot\omega\cdot r_{inner}^4}\right)^{0.25} \tag{7}$$

$$mass=\Pi\cdot(r_{outer}^2-r_{inner}^2)\cdot height\cdot\rho \tag{8}$$

Stress Analysis

The tangential and radial stresses, as a function of radius, induced in a constant thickness rim subjected to a constant angular velocity are given below. Both of these stresses are tensile due to the spinning nature of the rim. A complete derivation of these formulae may be found elsewhere (6). The stresses are incrementally calculated starting at the inner radius.

$$\sigma_{tang}(r)=\rho\cdot\omega^2\cdot r_{outer}^2\cdot\left(\frac{3+\nu}{9-\mu^2}\right)\cdot\left[\mu\cdot L\cdot\chi(r)^{\mu-1}+\mu\cdot(L-1)\cdot\chi(r)^{-(\mu+1)}-\left(\frac{\mu^2+3\nu}{3+\nu}\right)\cdot\chi(r)^2\right] \tag{9}$$

$$\sigma_{radial}(r)=\rho\cdot\omega^2\cdot r_{outer}^2\cdot\left(\frac{3+\nu}{9-\mu^2}\right)\cdot\left[L\cdot\chi(r)^{\mu-1}-(L-1)\cdot\chi(r)^{-(\mu+1)}-\chi(r)^2\right] \tag{10}$$

where,

$$\mu=\sqrt{\frac{E_{c11}}{E_{c22}}} \tag{11}$$

(12)

$$\chi(r)=\frac{r}{r_{outer}}$$

$$\beta=\frac{r_{inner}}{r_{outer}} \tag{13}$$

and,

$$L=\frac{\beta^{-(\mu+1)}-\beta^{2}}{\beta^{-(\mu+1)}-\beta^{\mu-1}} \tag{14}$$

For isotropic materials, $\mu = 1.0$, and $L = 1 + \beta^2$.

Failure Criteria

A failure criterion is needed to measure each material's effectiveness in the above spinning-induced stress fields. The following failure criterion (13-14) were considered to determine the amount of induced stress which causes the rim to fail: Maximum Stress Theory, Maximum Strain Theory, Maximum Strain Energy, Internal Friction Theory, and the Modified Distortion Energy Criterion. However, since 1) the rim's stress state is tensile-tensile (tensile in both the tangential and radial directions), and, 2) the maximum tangential stresses are two orders of magnitude greater than the maximum radial stresses in the rim (shown later); all of the above failure criterion yielded the same result. This agrees with previous findings (13). Therefore, due to it's simplicity the Maximum Stress Theory is used. Since the maximum tangential stresses occur at the inner radius ($\sigma_{tang}(r_{inner})$) the safety factor using the Maximum Stress Theory is defined as;

$$SAFETY\cdot FACTOR=\frac{S_{tang}}{\sigma_{tang}(r_{inner})} \tag{15}$$

For isotropic materials, $S_{tang} = S_{rad} = S_u$.

RESULTS AND DISCUSSION

The two main objectives of this work are: 1) to compare a number of composite materials to metals presently used in the construction of momentum wheels, and, 2) to determine which composite best meets the specified requirements while having the lowest

mass. A sample calculation follows.

A composite made of E-glass fibers (0.6 fiber volume ratio, no voids) and a high modulus matrix (HM) was considered. The resulting outer radius and total mass were calculated to be 0.321 meters (12.645 in) and 1.648 kg (3.633 lb_m), respectively. The tangential and radial stresses for this composite rim as a function of radius are seen in Figure 1. It is apparent that the tangential stresses are highest at the inner radius (79.3 MPa , 12 kpsi), whereas the radial stresses are negligible (maximum of 0.15 MPa, 20 psi). The relative shapes and magnitudes of these curves are typical of the other materials. By dividing the tangential strength of the composite (1656 MPa, 240 kpsi) by the maximum tangential stress, it was found that this composite rim had a safety factor of 20.9.

The resulting calculations using a fiber volume ratio of 0.6 and assuming no voids for the remaining eleven composites, together with the isotropic metals considered are summarized in Table 4.

Some significant points can be drawn from Table 4.

* Each of the composite materials has much higher safety factors than any of the isotropic metals evaluated, while being less massive.
* Primarily due to their lower density, the maximum tangential stress of each composite is lower than that of the isotropic materials'.
* The maximum tangential stress of the cast iron rim is nearly twice its ultimate strength (Safety Factor of 0.52), and the carbon steel rim is near failure (safety factor of 1.2). These results show conclusively why the high performance metals are used instead of these more common, less expensive metals.

Perhaps the most interesting result to come out of the above calculations is the fact that the fiber volume ratios of the composite systems may be varied, allowing the rim to be less massive while constrained to the same angular momentum at the same angular velocity. By changing the fiber volume ratio, the safety factor, mass, outer radius and maximum tangential stress of the free-standing rim were altered. The fact that the isotropic materials can not be altered is an obvious but equally important point.

The results of varying the fiber volume ratio for each composite system considered can be seen in Figures 2 through 13. The safety factor, mass, outer radius, and maximum tangential stress plotted vs. the fiber volume ratio are presented. As seen, since the matrix is both less dense and has lower strength, both the mass and safety factor decrease as the fiber volume ratio is decreased. The volume of the rim must increase, thus, the outer radius must increase, as the fiber volume ratio is decreased to counter the resulting decrease in rim density.

The usefulness of these figures is shown by example. Say that it is desired to make a free-standing rim out of Kevlar fibers and a high modulus (HM) matrix that will meet the design constraints set forth in this study. Say also that a safety factor of 18 is desired. Looking at Part A of Figure 7, a safety factor of 18 corresponds to a fiber volume ratio of $\sim$0.36. With this fiber volume ratio it is a simple matter to obtain the mass ($\sim$1.6 kg, 3.5

lb_m), outer radius (~0.33 m, 13.01 in), and the maximum stress applied to the rim (~55 MPa, 8.0 ksi) using the three other accompanying figures. Thus, the entire geometry, mass and maximum stress conditions are known for the rim that satisfy the given dynamic requirements. These figures are also useful if a design must meet certain outer radius or mass requirements.

Figure 14 shows the safety factor as a function of mass for the twelve composites systems. Part A couples the six fibers with the HM matrix, whereas Part B couples the six fibers with the IMHS matrix. The resulting data of the 18 Ni-250 (maraging) steel is included for comparison. As indicated on the E-Glass/HM composite system, the fiber volume ratio increases as the curves proceed from left to right. Each data point indicates a fiber volume ratio incremented by 0.1 (0.0 to 0.7).

Since it is desirable to have the lightest rim at a given safety factor, the slopes of these curves represent the composites' effectiveness in meeting the design criteria. A large slope indicates that the composite system weighs less at a desired safety factor than does a composite with a smaller slope. The two figures indicate that the composites utilizing Kevlar fibers have the greatest slopes, and thus are the least massive at any given safety factor. The carbon fiber (AS and T300) composites are the next most effective composite systems, followed by S-glass and boron. The E-Glass composites have the smallest slopes, and therefore, are the most massive of the composite systems considered at any given safety factor.

The results also indicate that each of the twelve composites, at any fiber volume ratio, is less massive than maraging steel, and that for a fiber volume ratio greater than ~0.2 each composite has a higher safety factor than maraging steel.

SUMMARY

This preliminary study shows that each of the twelve unidirectional-fiber composites considered meet the geometric and dynamic constraints set forth in the study with higher safety factors and less mass than any of the isotropic materials considered for fiber volume ratios of 0.2 or greater. For example, at a fiber volume ratio of 0.6, the Kevlar/IMHS composite system has a safety factor 4.5 times greater than that of the maraging steel system and a ~10% reduction in weight. If mass is the primary concern, a Kevlar fiber composite meets the requirements with the least mass regardless of fiber volume ratio while still having a high safety factor.

REFERENCES

1. Kirk, J.A., and Studer, P.A.: "Flywheel Energy Storage-II, Magnetically Suspended Superflywheel," Int. J. Mech. Sci., V. 19, 1977, pp. 233-245.
2. Post, R.F., and Post, S.F.: "Flywheels," Scientific American, V. 229, N. 6, Dec. 1973, pp. 17-23.
3. Gentra, G.: Kinetic Energy Storage, Butterworth & Co., 1985.
4. Kirk, J.A., and Huntington, R.A.: "Energy Storage - An Interference Assembled Multiring Superflywheel," 12th IECEC, V. 1, 1977, pp. 517-524.
5. Ashland, S.: "Flywheels put a New Spin on Electric Vehicles," Mech. Eng., Oct. 1993, pp. 44-51.
6. Ries, D.M. and Kirk, J.A.: "Manufacturing Analysis of Composite Multi-Ring Flywheel," Aerospace Eng., Oct. 1992, pp. 14-18.
7. Chamis, C.C.: "Simplified Composite Micromechanics Equations for Hygral, Thermal, and Mechanical Properties," SAMPE Quarterly, April 1984, pp. 14-23.
8. Chamis, C.C.: "Simplified Composite Micromechanics Equations for Strength, Fracture Toughness, and Environmental Effects," SAMPE Quarterly, July 1984, pp. 41-55.
9. Heimel, H.,: "Evolution of Large Momentum and Reaction Wheels," ESA SP-279, Dec. 1987, pp. 297-302.
10. Gauthier, M., Roland, J.P., Vaillant, H., and Robinson, A.A.: "An Advanced Low-Cost 2-Axis Active Magnetic Bearing Flywheel," ESA SP-279, Dec. 1987, pp. 177-182.
11. Eckardt, T.: "The Low Noise Momentum Wheel MW-X EM Design and Predicted Properties," ESA SP-334, April 1993, pp. 263-268.
12. Wyn-Roberts, D.: "Space Mechanisms Development in the ESA Technological Research Programme," ESA SP-231, Oct. 1985, pp. 305-311.
13. Nahas, M.N.: "Survey of Failure and Post-Failure Theories of Laminated Fiber-Reinforced Composites," J. Composites Tech. & Research, V. 8, N. 4, Winter 1986, pp. 138-153.
14. Chamis, C.C.: "Prediction of Fiber Composite Mechanical Behavior Made Simple," NASA TM-81404, 1980.

APPENDIX I

Nomenclature

r_{inner}	Inner radius of the rim, [m]
r_{outer}	Outer radius of the rim, [m]
height	Height of the rim, [m]
mass	Mass of the rim meeting the set constraints, [kg]
ω	Angular velocity of the rim, [rad/sec]
H	Angular momentum of the rotating rim, [N*m*sec]
Safety Factor	= Tangential strength of the rim divided by the maximum tangential stress of the rim design, [-]
k_f	Fiber volume ratio, [-]
k_m	Matrix volume ratio, [-]
ρ	Density of either the metal or the composite system, [kg/m^3]
ρ_f	Density of the fiber, [kg/m^3]
ρ_m	Density of the matrix, [kg/m^3]
ν	Poisson's ratio of either the metal or of the composite, [-]
ν_{c12}	Composite longitudinal Poisson's ratio, [-]
ν_{f12}	Fiber longitudinal Poisson's ratio, [-]
ν_m	Matrix Poisson's ratio, [-]
E_{tang}, E_{c11}	Tangential Modulus of Elasticity of the composite, [GPa]
E_{f11}	Longitudinal Modulus of Elasticity of the fiber, [GPa]
E_m	Modulus of Elasticity of the matrix, [GPa]
E_{rad}, E_{c22}	Radial Modulus of Elasticity of the composite, [GPa]
E_{f22}	Transverse Modulus of Elasticity of the fiber, [GPa]
S_u	Ultimate strength, [MPa]
S_{tang}, S_{c11}	Tangential strength of the composite, [MPa]
S_{f11}	Longitudinal strength of the composite, [MPa]
S_{rad}	Radial strength of the composite, [MPa]
$\sigma_{tang}(r)$	Tangential stress as a function of radius, [MPa]
$\sigma_{tang}(r_{inner})$	Maximum tangential stress, which occurs at the inner radius, [MPa]
$\sigma_{radial}(r)$	Radial stress as a function of radius, [MPa]
μ, L, β	Simplicity factors for stress calculations, [-]
$\chi(r)$	Simplicity factor for stress calculation dependant upon radius, [-]

Table 1. Properties of the conventional (metal) materials considered in the study. Values, in part, taken from (6).

Material	Density, ρ [X 10^3 kg/m^3]	Poisson's Ratio, ν	Ultimate Strength, S_u [MPa]
Titanium Alloy (ZK 60)	5.111	0.3	1150
AISI 4340	7.830	0.32	1790
18 Ni-250 (maraging)	8.000	0.3	1860
hp 9-4-20	7.830	0.296	1480†
hp 9-4-30	7.830	0.296	1660‡
Cast Iron (G15)	7.895	0.3	150
Carbon Steel (Fe 34)	7.727	0.3	340

† Values ranged from 1310 to 1480 MPa (6).
‡ Values ranged from 1520 to 1660 MPa (6).

Table 2. Properties of the 6 fiber (7,8).

Fiber Type	Density, ρ_f [X 10^3 kg/m^3]	Longitudinal Modulus of Elasticity, E_{f11} [GPa]	Transverse Modulus of Elasticity, E_{f22} [GPa]	Longitudinal Poisson's Ratio, ν_{f12}	Longitudinal Tensile Stress, S_{f11} [MPa]
E-Glass	2.49	73	73	0.22	2760
S-Glass	2.49	85	85	0.2	4140
Boron	2.63	400	400	0.2	4140
AS	1.74	215	14	0.2	2070
T300	1.77	220	14	0.2	2410
Kevlar	1.47	150	4.1	0.35	2760

Table 3. Properties of the 2 matrix types (7,8).

Matrix Type	Density, ρ_m [X 10^3 kg/m^3]	Modulus of Elasticity, E_m [GPa]	Poisson's Ratio, ν_m
High Modulus (HM)	1.246	5.2	0.35
Intermediate Modulus High Strength (IMHS)	1.218	3.4	0.35

Table 4. Calculation summary for the twelve composites using a fiber volume ratio of 0.6, and the seven isotropic metals.

Material	Safety Factor	Mass, [kg]	Outer Radius, r_{outer} [m]	Maximum Tang. Stress, $\sigma_{tang}(r_{inner})$ [MPa]
E-Glass/HM	20.9	1.648	0.321	79.3
Boron/HM	30.2	1.642	0.320	82.2
S-Glass/HM	31.4	1.648	0.321	79.2
AS/HM	19.6	1.619	0.327	63.3
T300/HM	22.9	1.619	0.327	63.3
Kevlar/HM	28.7	1.604	0.329	57.6
E-Glass/IMHS	20.9	1.648	0.321	79.3
Boron/IMHS	30.2	1.652	0.320	82.2
S-Glass/IMHS	31.3	1.648	0.321	79.2
AS/IMHS	19.9	1.617	0.327	62.3
T300/IMHS	22.9	1.619	0.327	63.3
Kevlar/IMHS	29.3	1.601	0.330	56.5
Titanium Alloy (ZK 60)	6.0	1.717	0.309	190.5
AISI 4340	6.2	1.734	0.306	287.2
18 Ni-250 (maraging)	6.3	1.735	0.306	293.2
hp 9-4-20	5.2	1.734	0.306	287.2
hp 9-4-30	5.8	1.734	0.306	287.2
Cast Iron (G15)	**0.52**	1.735	0.306	289.5
Carbon Steel (Fe 34)	1.2	1.734	0.306	283.5

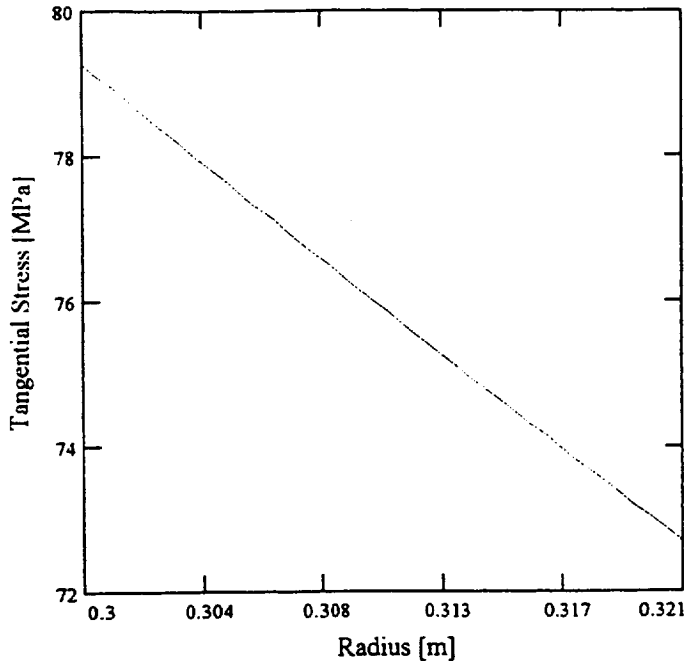

Part A: Tangential Stress vs. Radius

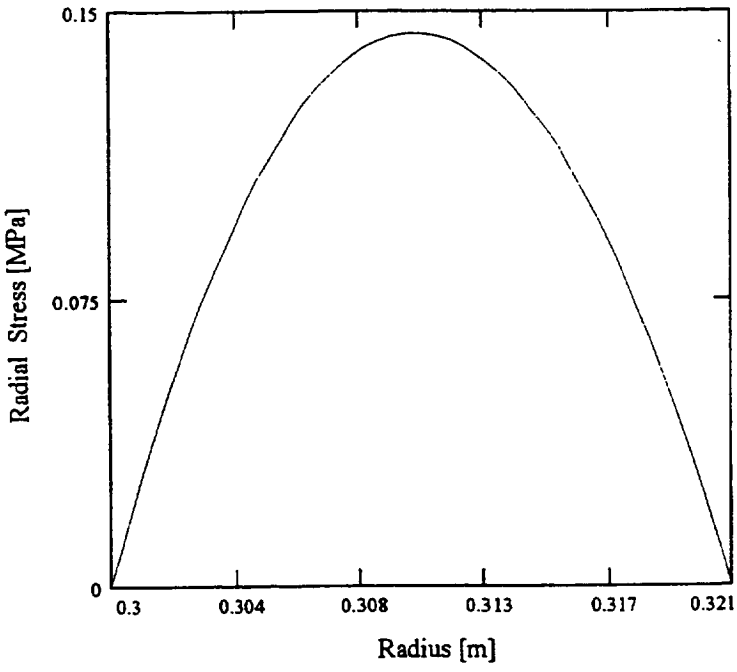

Part B: Radial Stress vs. Radius

Figure 1. Stress vs. Radius for the E-Glass/ HM Epoxy Composite

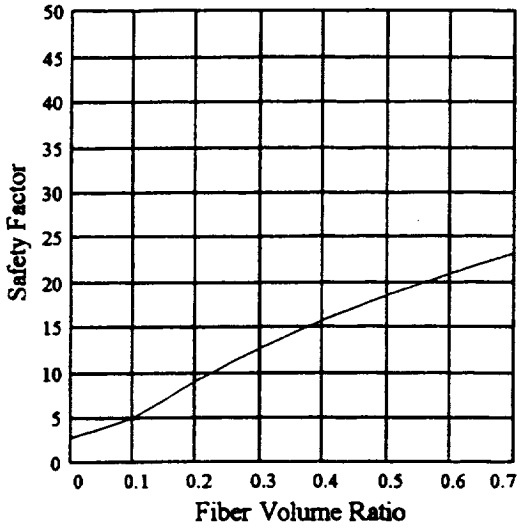

Part A: Safety Factor vs. Fiber Volume Ratio

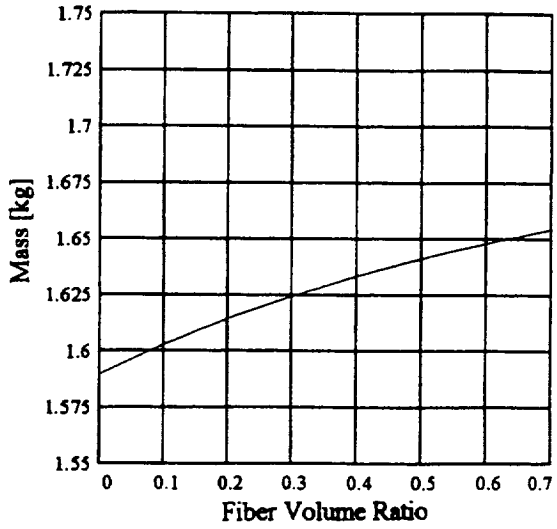

Part B: Rim Mass vs. Fiber Volume Ratio

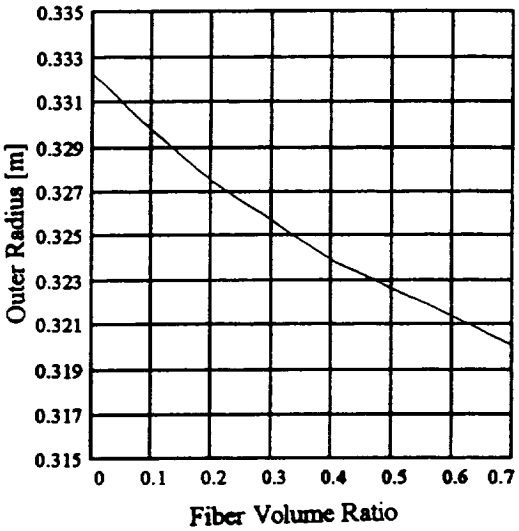

Part C: Outer Radius vs. Fiber Volume Ratio

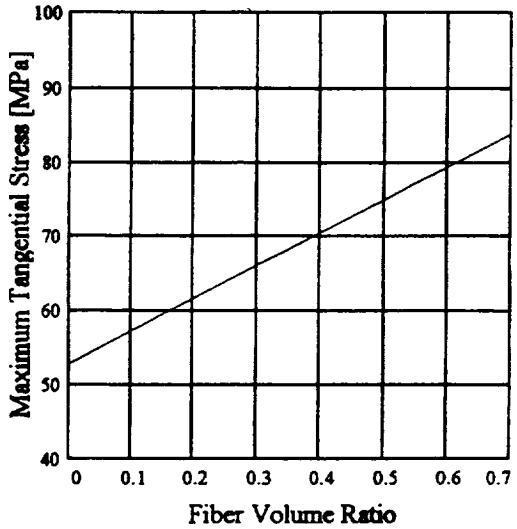

Part D: Maximum Tang. Stress vs. Fiber Volume Ratio

Figure 2. E-Glass/HM Epoxy Composite

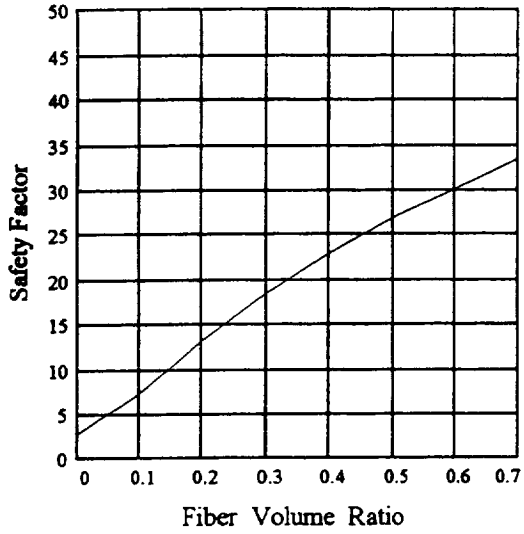

Part A: Safety Factor vs. Fiber Volume Ratio

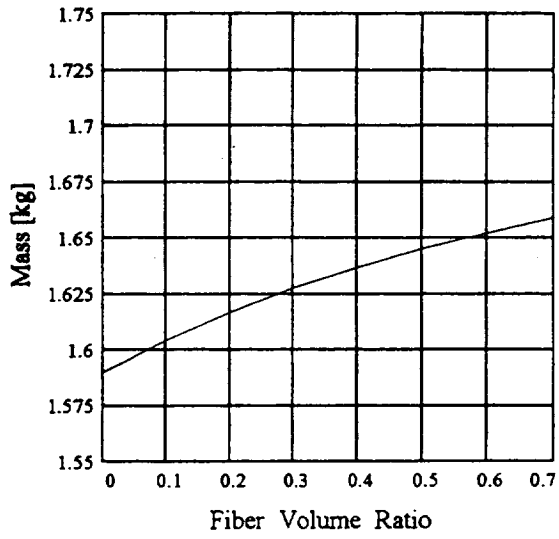

Part B: Rim Mass vs. Fiber Volume Ratio

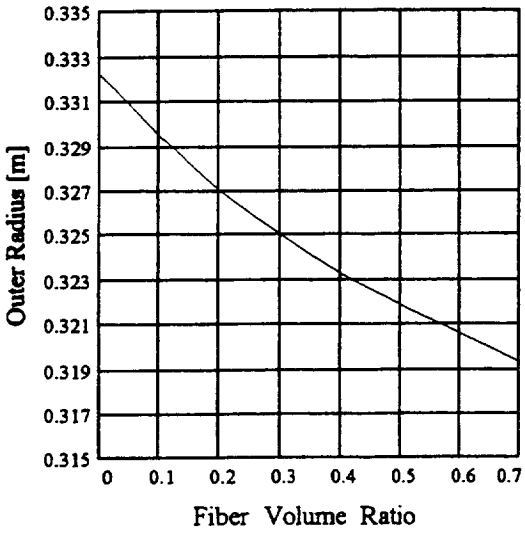

Part C: Outer Radius vs. Fiber Volume Ratio

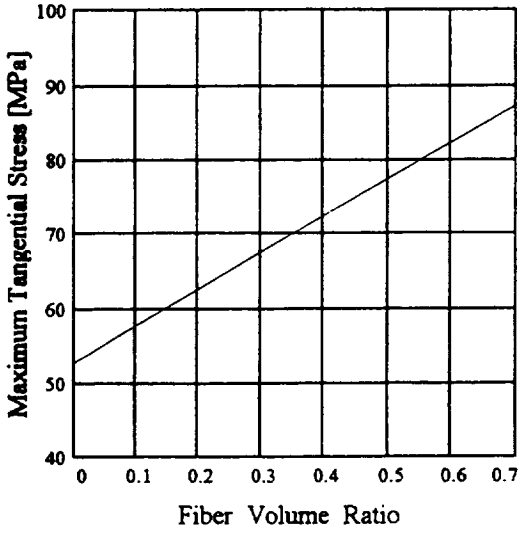

Part D: Maximum Tang. Stress vs. Fiber Volume Ratio

Figure 3. Boron/HM Epoxy Composite

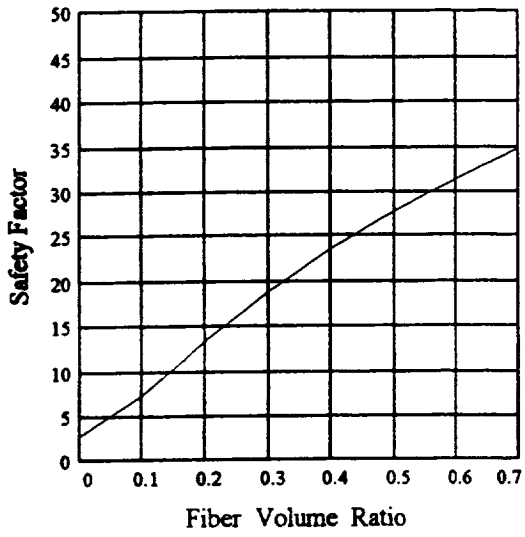

Part A: Safety Factor vs. Fiber Volume Ratio

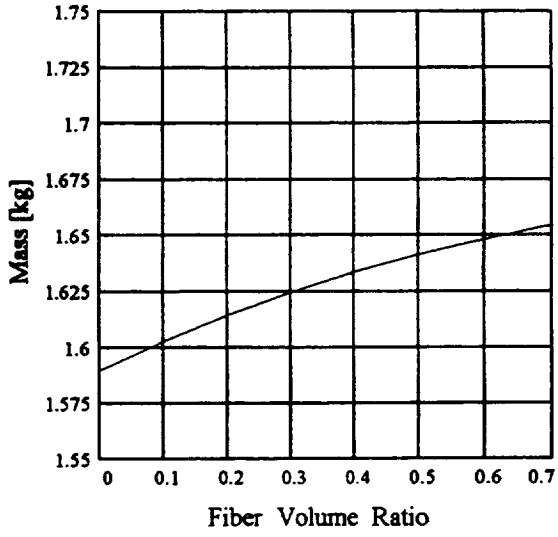

Part B: Rim Mass vs. Fiber Volume Ratio

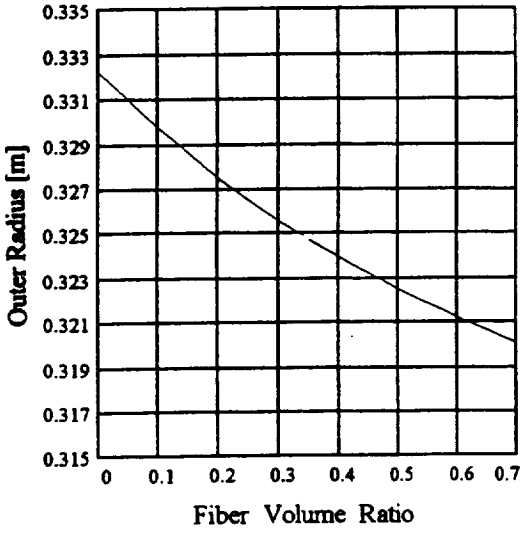

Part C: Outer Radius vs. Fiber Volume Ratio

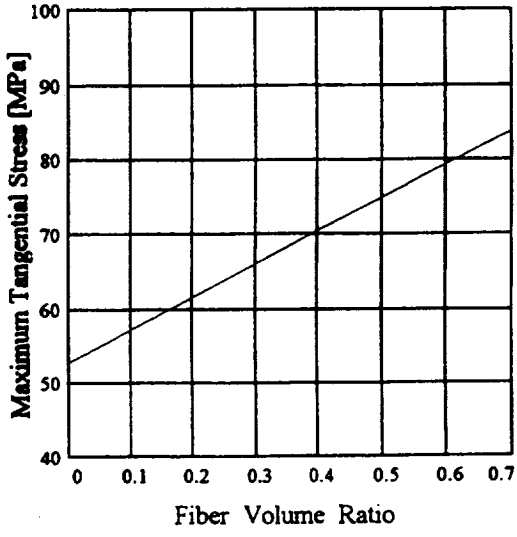

Part D: Maximum Tang. Stress vs. Fiber Volume Ratio

Figure 4. S-Glass/HM Epoxy Composite

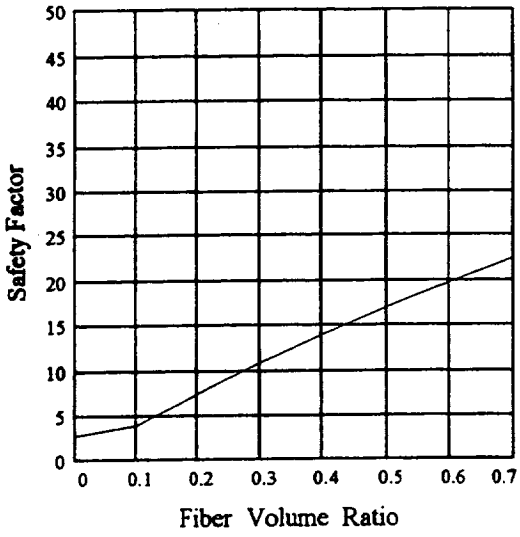

Part A: Safety Factor vs. Fiber Volume Ratio

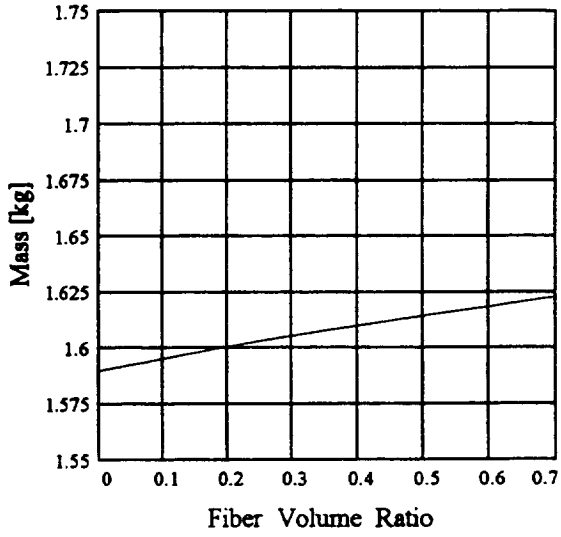

Part B: Rim Mass vs. Fiber Volume Ratio

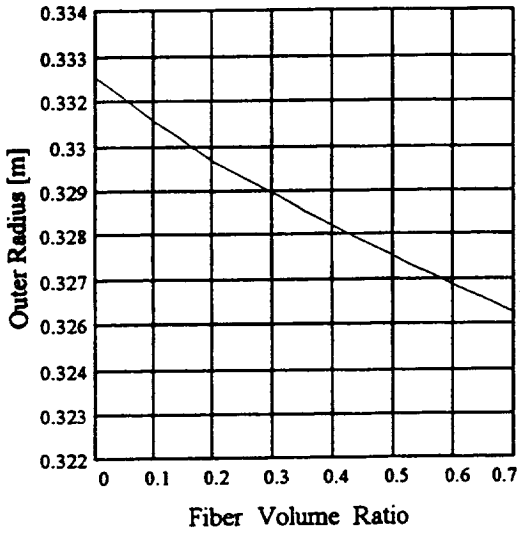

Part C: Outer Radius vs. Fiber Volume Ratio

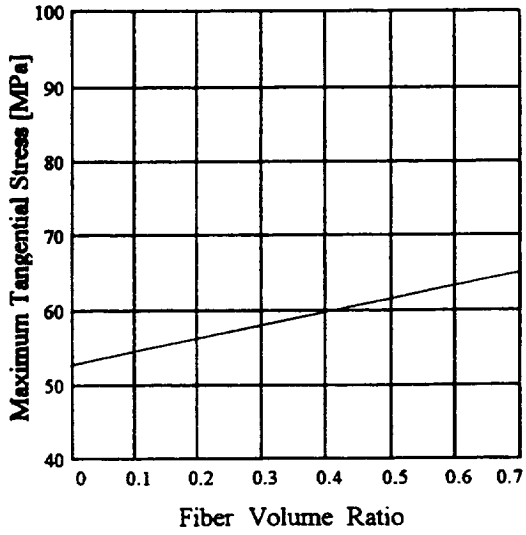

Part D: Maximum Tang. Stress vs. Fiber Volume Ratio

Figure 5. AS/HM Epoxy Composite

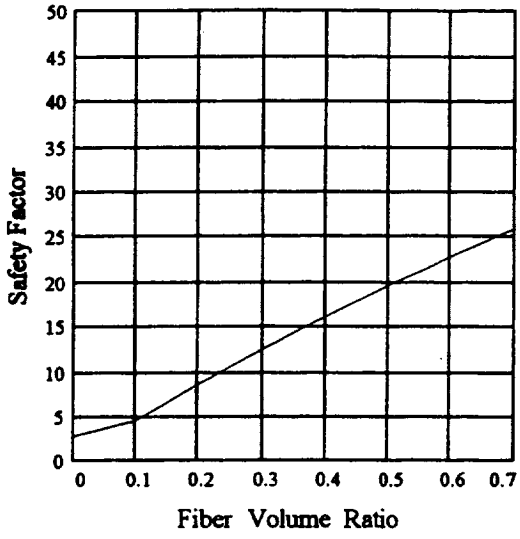

Part A: Safety Factor vs. Fiber Volume Ratio

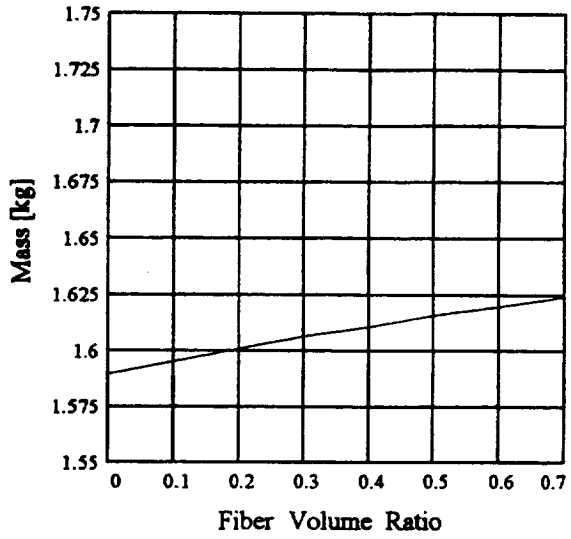

Part B: Rim Mass vs. Fiber Volume Ratio

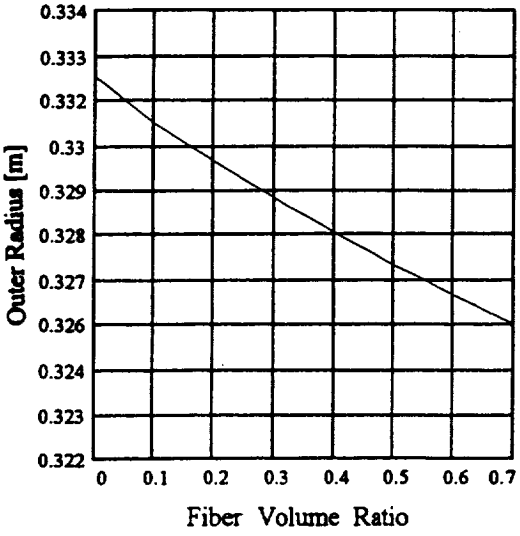

Part C: Outer Radius vs. Fiber Volume Ratio

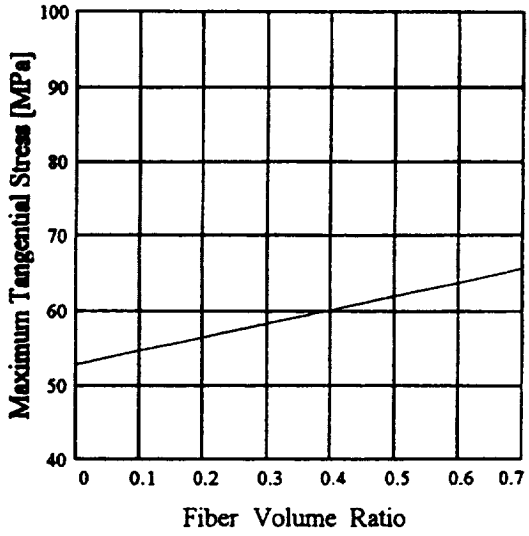

Part D: Maximum Tang. Stress vs. Fiber Volume Ratio

Figure 6. T300/HM Epoxy Composite

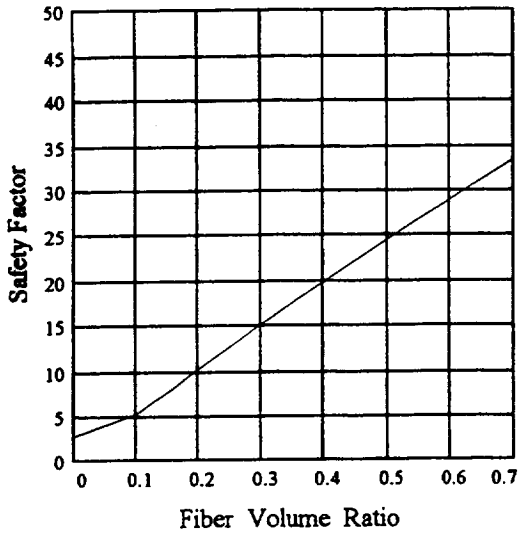

Part A: Safety Factor vs. Fiber Volume Ratio

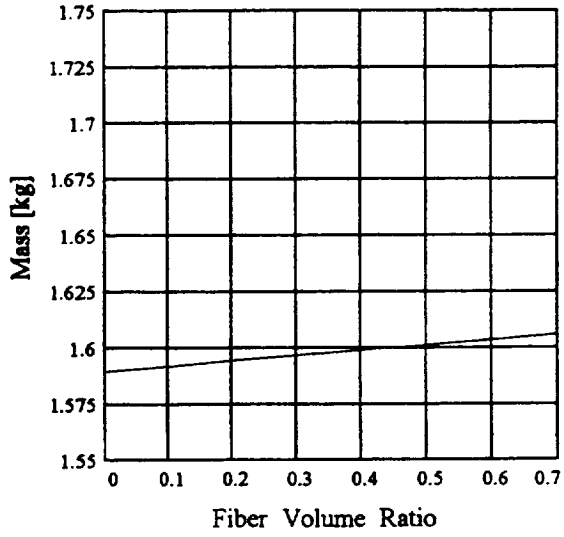

Part B: Rim Mass vs. Fiber Volume Ratio

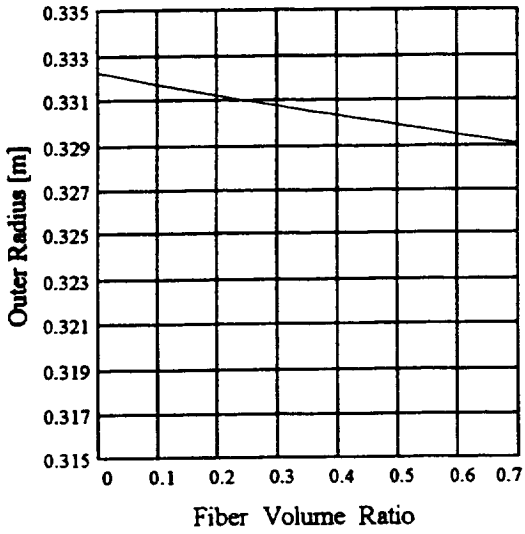

Part C: Outer Radius vs. Fiber Volume Ratio

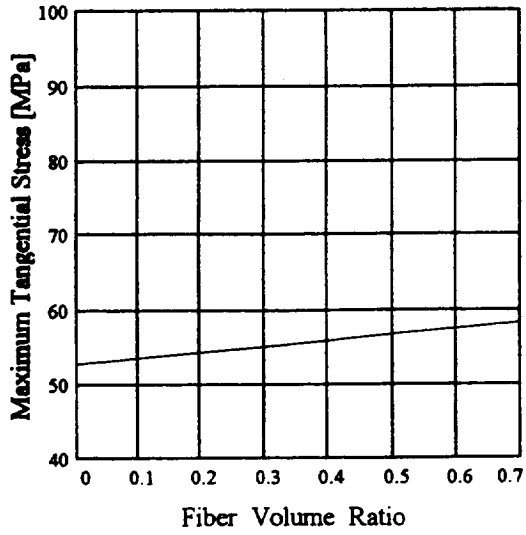

Part D: Maximum Tang. Stress vs. Fiber Volume Ratio

Figure 7. Kevlar/HM Epoxy Composite

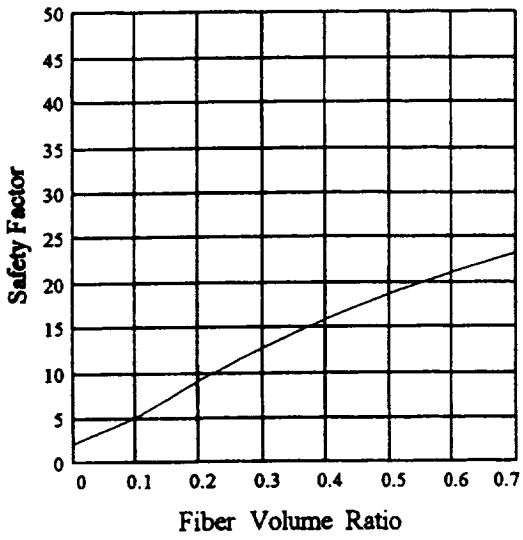

Part A: Safety Factor vs. Fiber Volume Ratio

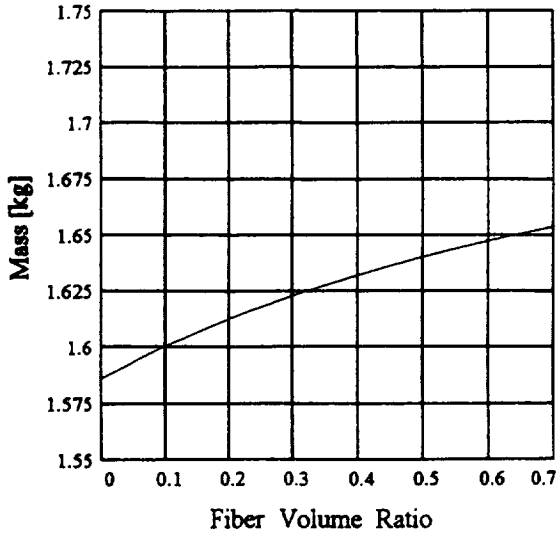

Part B: Rim Mass vs. Fiber Volume Ratio

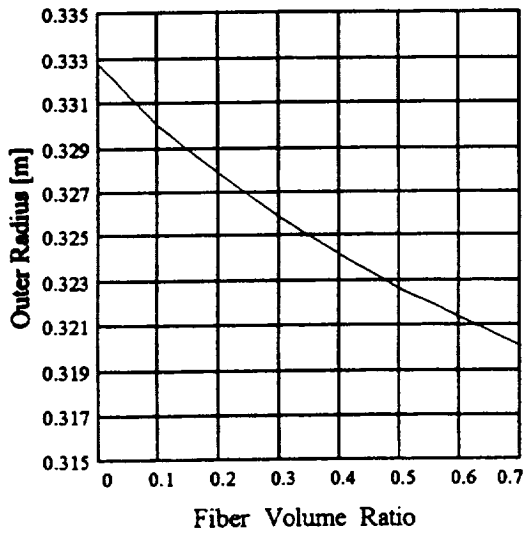

Part C: Outer Radius vs. Fiber Volume Ratio

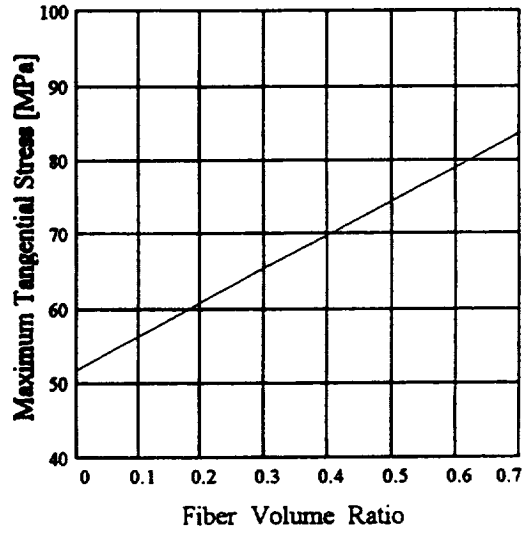

Part D: Maximum Tang. Stress vs. Fiber Volume Ratio

Figure 8. E-Glass/IMHS Epoxy Composite

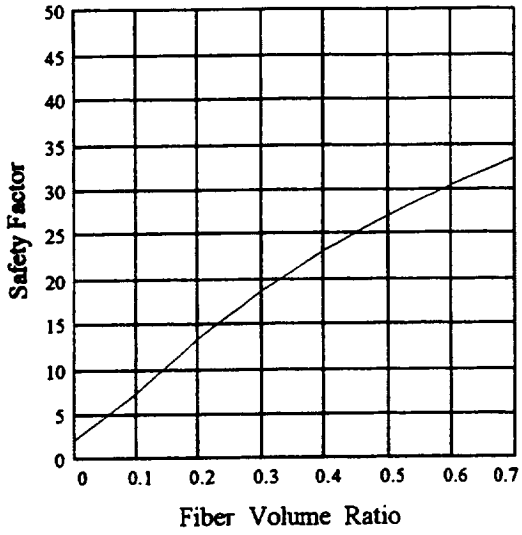

Part A: Safety Factor vs. Fiber Volume Ratio

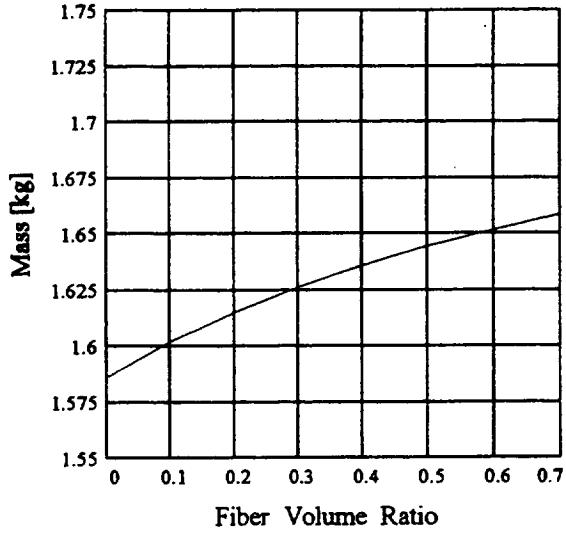

Part B: Rim Mass vs. Fiber Volume Ratio

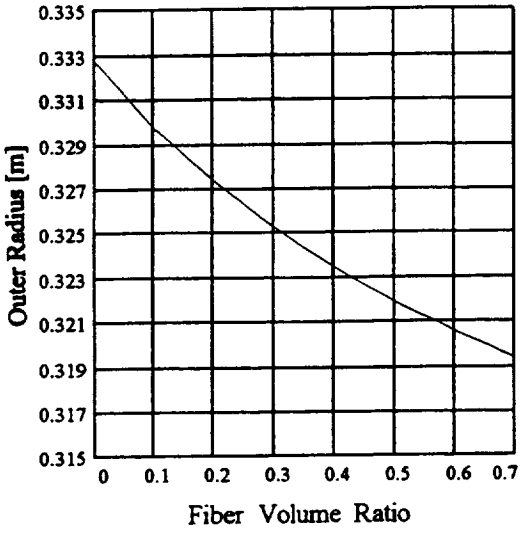

Part C: Outer Radius vs. Fiber Volume Ratio

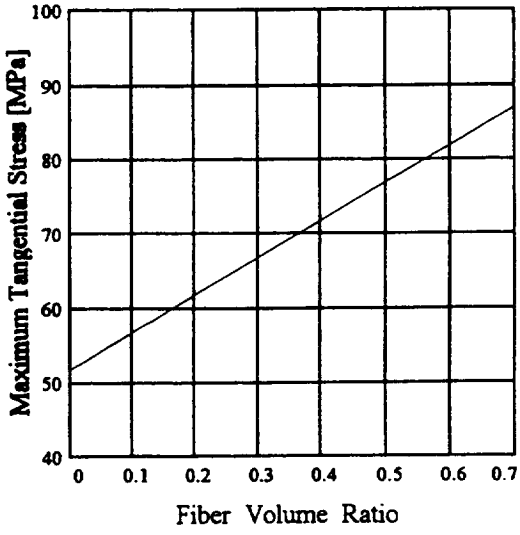

Part D: Maximum Tang. Stress vs. Fiber Volume Ratio

Figure 9. Boron/IMHS Epoxy Composite

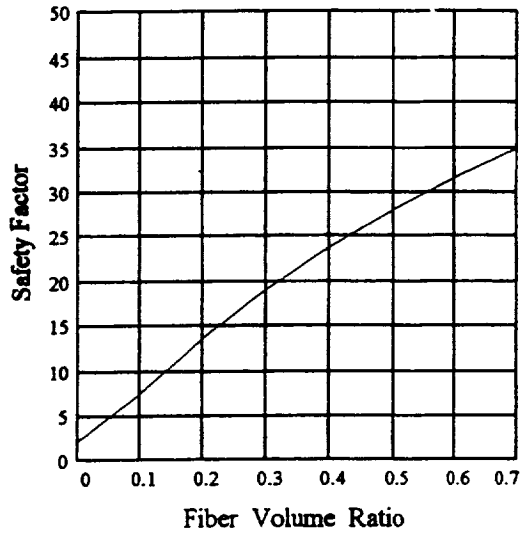

Part A: Safety Factor vs. Fiber Volume Ratio

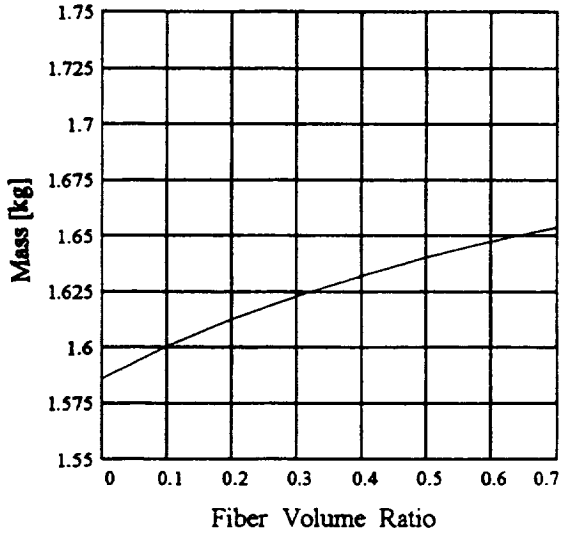

Part B: Rim Mass vs. Fiber Volume Ratio

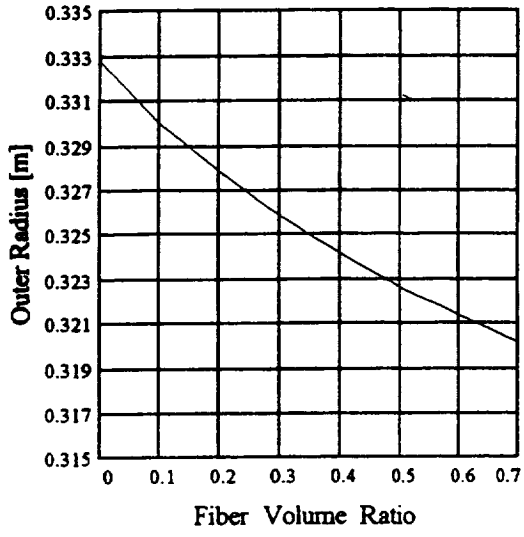

Part C: Outer Radius vs. Fiber Volume Ratio

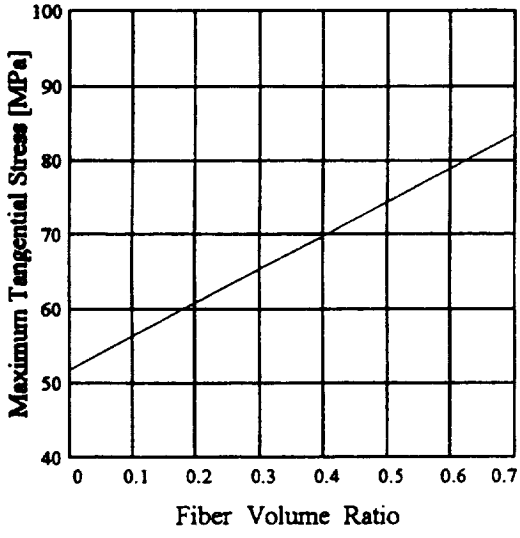

Part D: Maximum Tang. Stress vs. Fiber Volume Ratio

Figure 10. S-Glass/IMHS Epoxy Composite

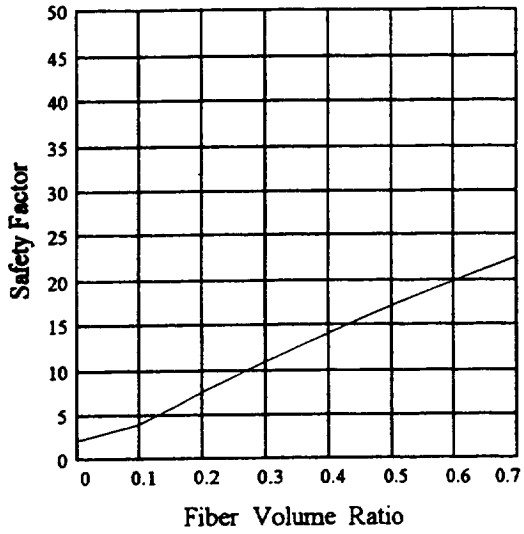

Part A: Safety Factor vs. Fiber Volume Ratio

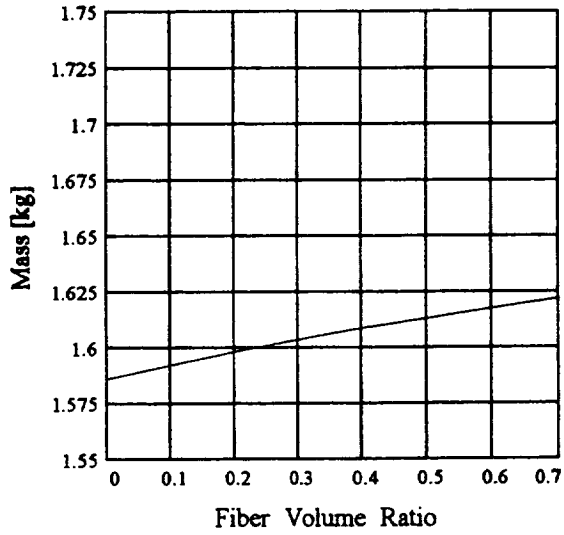

Part B: Rim Mass vs. Fiber Volume Ratio

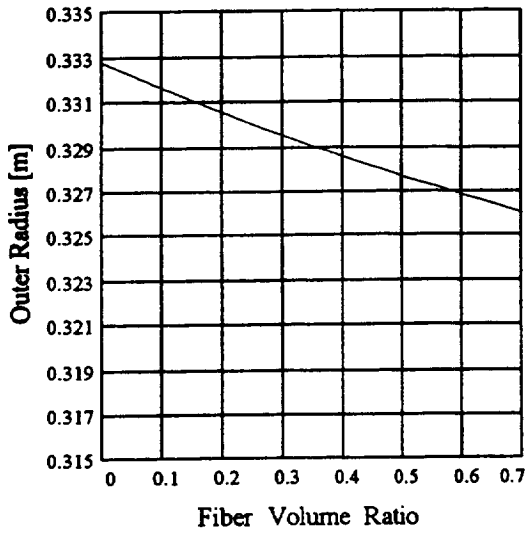

Part C: Outer Radius vs. Fiber Volume Ratio

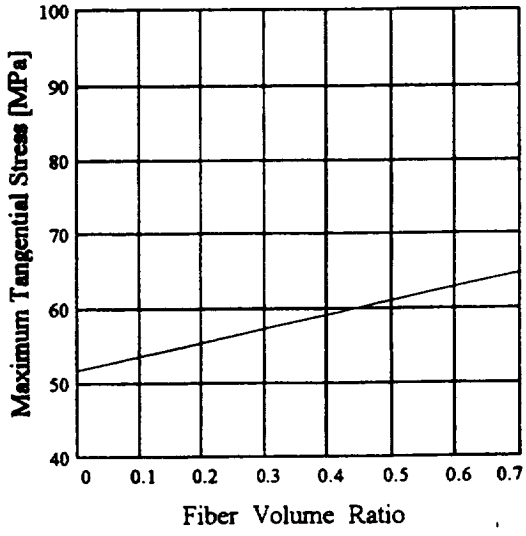

Part D: Maximum Tang. Stress vs. Fiber Volume Ratio

Figure 11. AS/IMHS Epoxy Composite

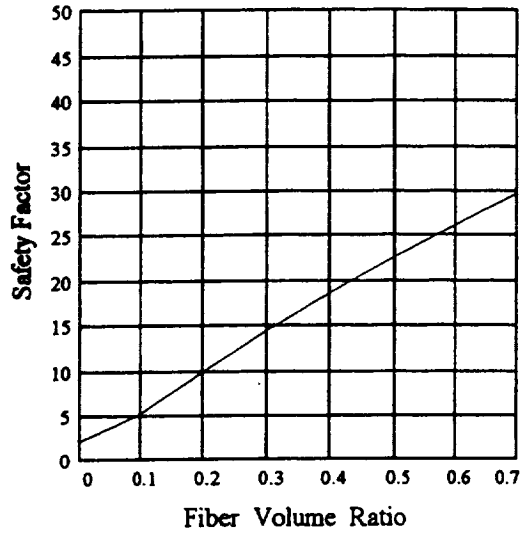

Part A: Safety Factor vs. Fiber Volume Ratio

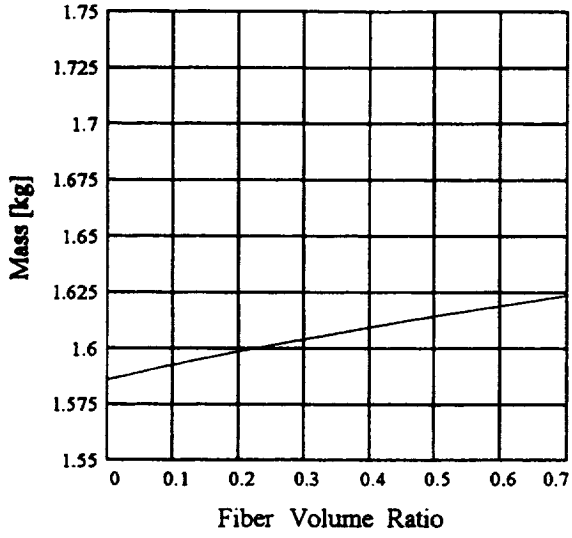

Part B: Rim Mass vs. Fiber Volume Ratio

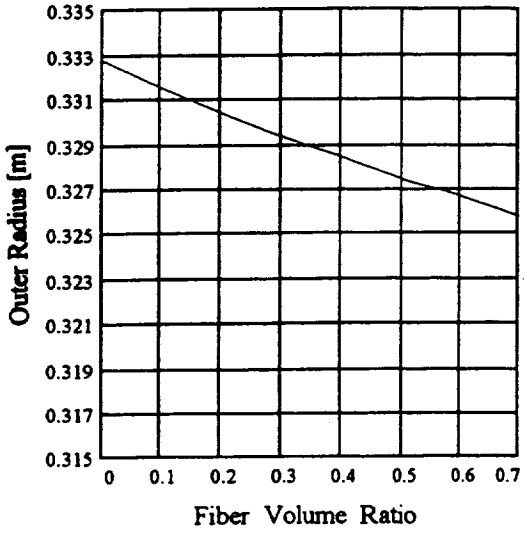

Part C: Outer Radius vs. Fiber Volume Ratio

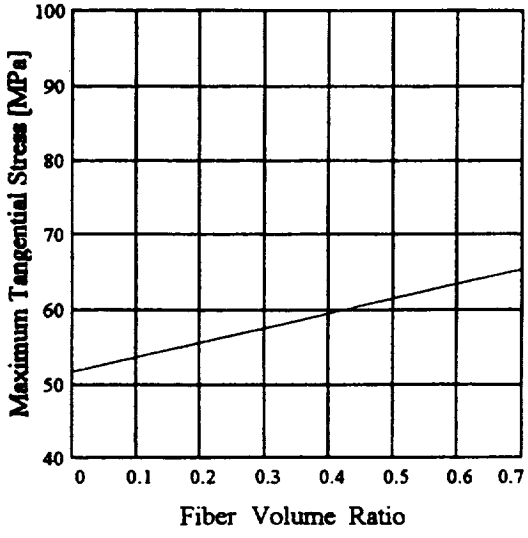

Part D: Maximum Tang. Stress vs. Fiber Volume Ratio

Figure 12. T300/IMHS Epoxy Composite

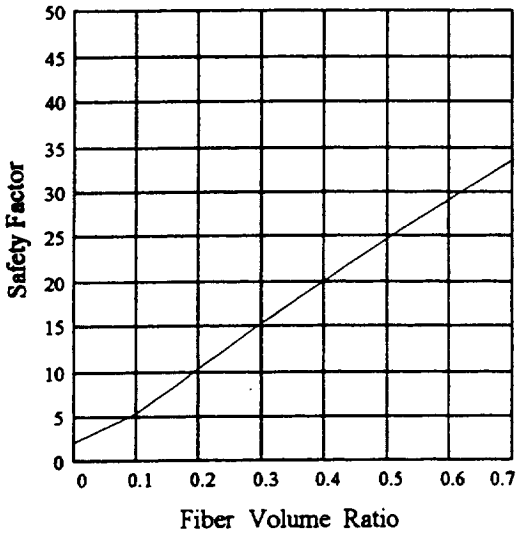

Part A: Safety Factor vs. Fiber Volume Ratio

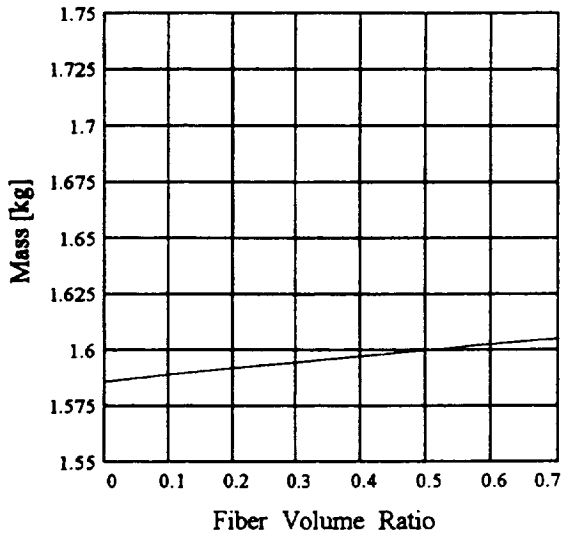

Part B: Rim Mass vs. Fiber Volume Ratio

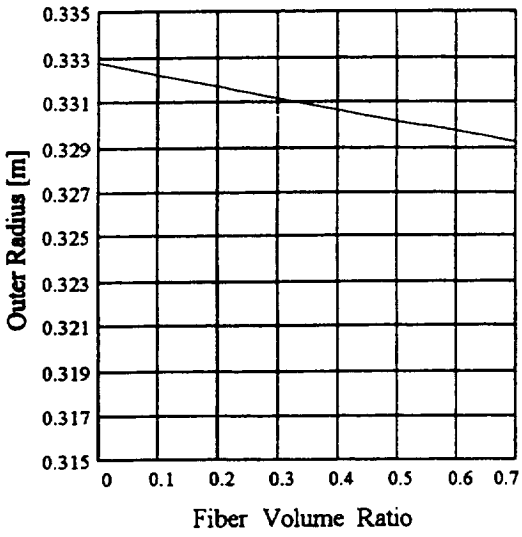

Part C: Outer Radius vs. Fiber Volume Ratio

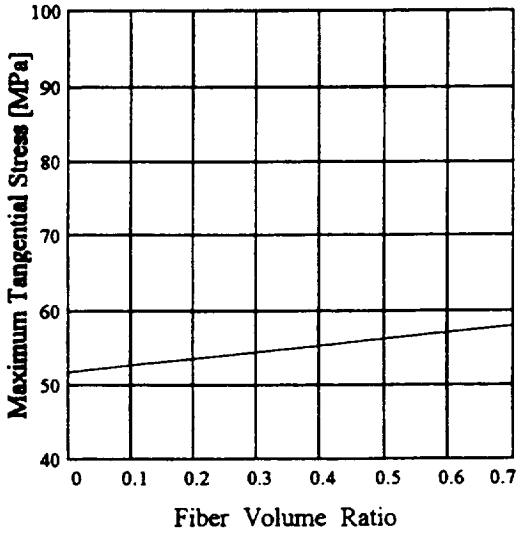

Part D: Maximum Tang. Stress vs. Fiber Volume Ratio

Figure 13. Kevlar/IMHS Epoxy Composite

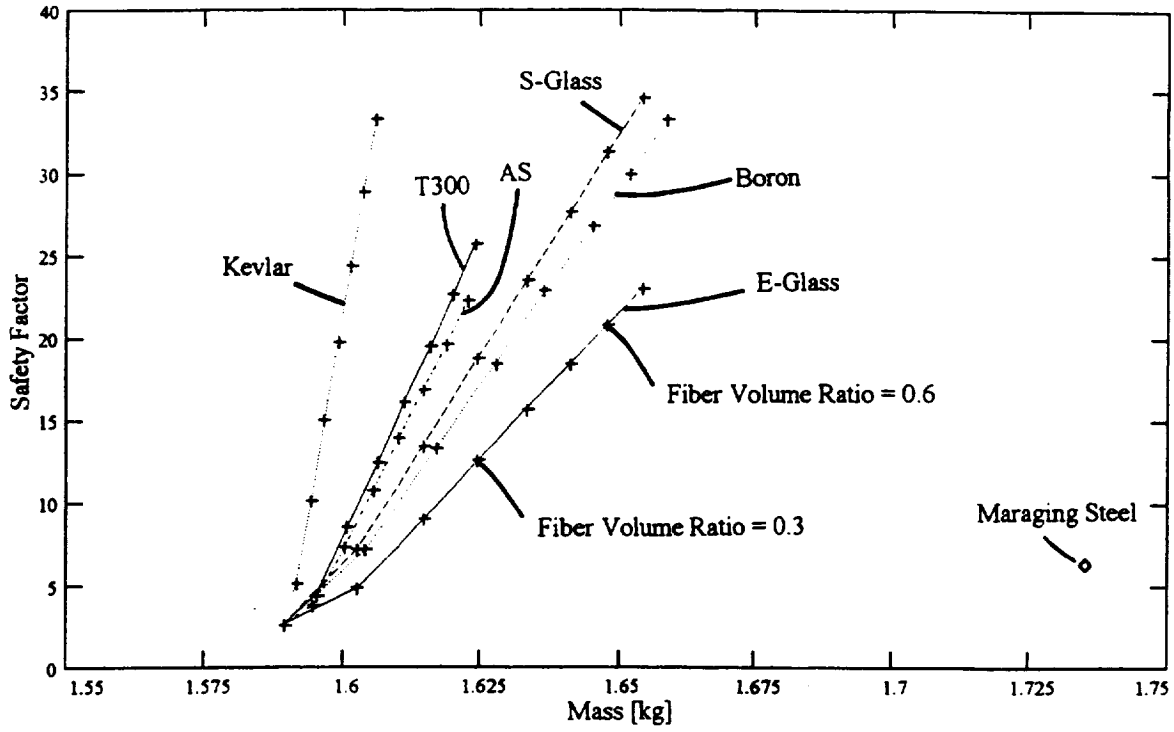

Part A. Safety Factor as a Function of Mass for the HM Composites.

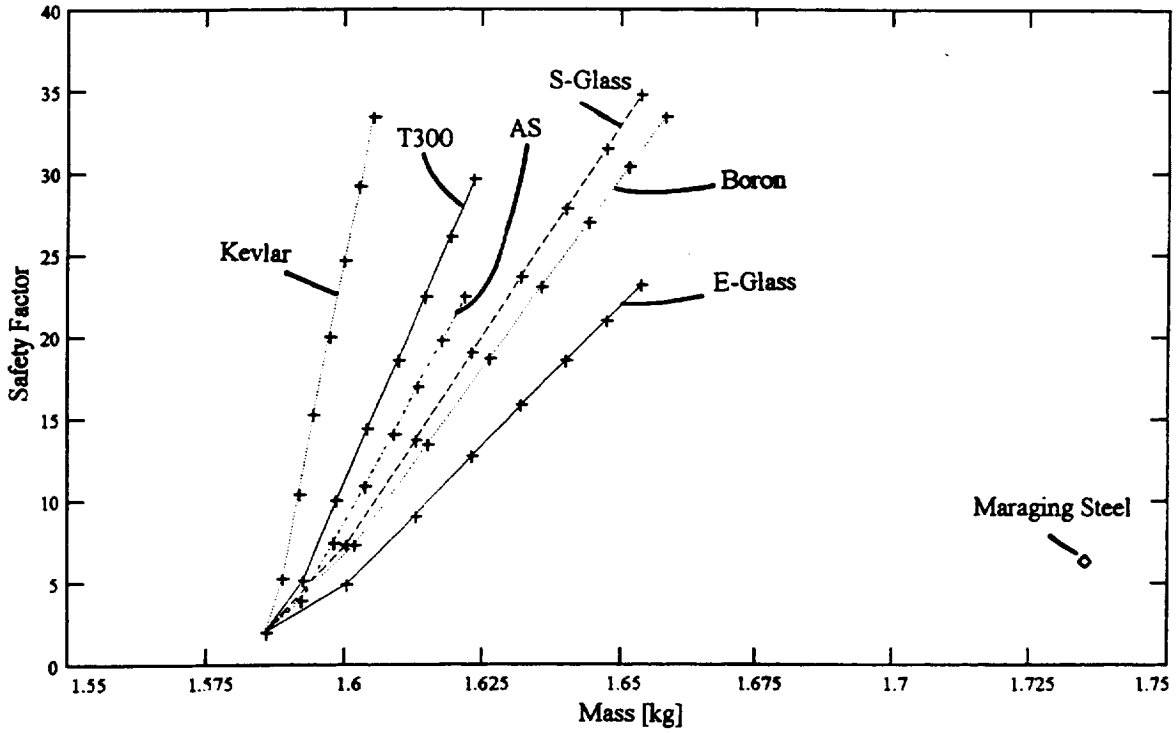

Part B. Safety Factor as a Function of Mass for the IMHS Composites.

Figure 14. Safety Factor vs. Mass of the Rim.

REPORT DOCUMENTATION PAGE

Form Approved
OMB No. 0704-0188

1. AGENCY USE ONLY (*Leave blank*)	2. REPORT DATE	3. REPORT TYPE AND DATES COVERED
	May 1995	Technical Memorandum

4. TITLE AND SUBTITLE

Design of a Unidirectional Composite Momentum Wheel Rim

5. FUNDING NUMBERS

WU-274-00-00

6. AUTHOR(S)

Bradley Shogrin, William R. Jones, Jr. and Joseph M. Prahl

7. PERFORMING ORGANIZATION NAME(S) AND ADDRESS(ES)

National Aeronautics and Space Administration
Lewis Research Center
Cleveland, Ohio 44135-3191

8. PERFORMING ORGANIZATION REPORT NUMBER

E-9613

9. SPONSORING/MONITORING AGENCY NAME(S) AND ADDRESS(ES)

National Aeronautics and Space Administration
Washington, D.C. 20546-0001

10. SPONSORING/MONITORING AGENCY REPORT NUMBER

NASA TM-106911

11. SUPPLEMENTARY NOTES

Bradley Shogrin and Joseph M. Prahl, Case Western Reserve University, Department of Mechanical Engineering, Cleveland, Ohio 44106; William R. Jones, Jr., NASA Lewis Research Center. Responsible person, William R. Jones, Jr., organization code 5140, (216) 433-6051.

12a. DISTRIBUTION/AVAILABILITY STATEMENT

Unclassified - Unlimited
Subject Category 18

This publication is available from the NASA Center for Aerospace Information, (301) 621-0390.

12b. DISTRIBUTION CODE

13. ABSTRACT ***(Maximum 200 words)***

A preliminary study comparing twelve unidirectional-fiber composite systems to five metal materials conventionally used in momentum wheels is presented. Six different fibers are considered in the study; E-Glass, S-Glass, Boron, AS, T300 and Kevlar. Because of the possibility of high momentum requirements, and, thus high stresses, only two matrix materials are considered; a high-modulus (HM) and a intermediate-modulus-high-strength (IMHS) matrix. Each of the six fibers are coupled with each of the two matrix materials. In an effort to optimize the composite system, each composite is considered while varying the fiber volume ratio from 0.0 to 0.7 in increments of 0.1. For fiber volume ratios above 0.2, all twelve unidirectional-fiber composite systems meet the study's requirements with higher factors of safety and less mass than the five conventional isotropic (metal) materials. For example, at a fiber volume ratio of 0.6, the Kevlar/IMHS composite system has a safety factor 4.5 times greater than that of a steel (maraging) system and a ~10% reduction in weight.

14. SUBJECT TERMS

Momentum wheel; Composite

15. NUMBER OF PAGES

29

16. PRICE CODE

A03

17. SECURITY CLASSIFICATION OF REPORT	18. SECURITY CLASSIFICATION OF THIS PAGE	19. SECURITY CLASSIFICATION OF ABSTRACT	20. LIMITATION OF ABSTRACT
Unclassified	Unclassified	Unclassified	